

# MULTILEVEL PRECONDITIONING FOR RIDGE REGRESSION\*

JORIS TAVERNIER<sup>†</sup>, JAAK SIMM<sup>‡</sup>, KARL MEERBERGEN<sup>†</sup>, AND YVES MOREAU<sup>‡</sup>

**Abstract.** Solving linear systems is often the computational bottleneck in real-life problems. Iterative solvers are the only option due to the complexity of direct algorithms or because the system matrix is not explicitly known. Here, we develop a multilevel preconditioner for regularized least squares linear systems involving a feature or data matrix. Variants of this linear system may appear in machine learning applications, such as ridge regression, logistic regression, support vector machines and matrix factorization with side information. We use clustering algorithms to create coarser levels that preserve the principal components of the covariance or Gram matrix. These coarser levels approximate the dominant eigenvectors and are used to build a multilevel preconditioner accelerating the Conjugate Gradient method. We observed speed-ups for artificial and real-life data. For a specific data set, we achieved speed-up up to a factor 100.

**Key words.** Multilevel preconditioning, Machine learning, Clustering, Ridge regression, Large-scale, Tikhonov regularization, Krylov subspace methods

**AMS subject classifications.** 65F08, 65F22, 68T05, 68T10

**1. Introduction.** The computational bottleneck in Machine Learning applications is often solving a linear system. These systems are usually solved iteratively due to the complexity of direct algorithms. Here we focus on problems from machine learning with variations of a least squares linear system leading to the regularized normal equations

$$(X^T X + \beta I)\mathbf{w} = X^T \mathbf{b} \quad (1.1)$$

with  $\beta$  a given regularization parameter. The feature matrix  $X \in \mathbb{R}^{N \times F}$  consists of  $N$  data samples with  $F$  features. This matrix is often high-dimensional and sparse. Hence, Krylov subspace methods are appealing, since they only require the matrix-vector multiplication and not the matrix itself. The feature matrix  $X$  can be sparse but the matrix product  $X^T X$  in (1.1) generally is not.

The number of iterations required to reach a certain tolerance for Krylov subspace methods depends on the spectrum of the matrix, more specifically the distribution of the eigenvalues [14, 38]. The condition number of the matrix is often an adequate indication. The art of preconditioning aims at reducing the number of iterations by transforming the problem to an easier one. One simple approach is to divide the matrix by its main diagonal and is called Jacobi preconditioning [39, 14]. Diagonal or Jacobi preconditioning is often very efficient if the matrix is diagonally dominant. Other existing preconditioning techniques such as incomplete Cholesky factorization [19, 21] or incomplete LU factorization [33] are useless since the matrix product in our linear system is dense. It is possible that the covariance matrix or Gram matrix  $X^T X$  follows some special structure for which the inverse is sparse. In this case, the Sparse Approximate Inverse [2] can be computed based on this sparse structure. However, in general the inverse of the covariance matrix is also dense.

For the solution of partial differential equations (PDEs), geometric Multigrid [11] and its algebraic extensions are often successful [41, 37, 31]. The crucial concept is that the eigenvectors that slow down the convergence of iterative methods, can be

\*This work was supported Research Foundation - Flanders (FWO, No. G079016).

<sup>†</sup>Department of Computer Science, KU Leuven, [Joris.Tavernier@cs.kuleuven.be](mailto:Joris.Tavernier@cs.kuleuven.be), <https://people.cs.kuleuven.be/~joris.tavernier/>, [Karl.Meerbergen@cs.kuleuven.be](mailto:Karl.Meerbergen@cs.kuleuven.be).

<sup>‡</sup>Department of Electrical Engineering, ESAT - STADIUS, KU Leuven, [jaak.simm@esat.kuleuven.be](mailto:jaak.simm@esat.kuleuven.be), [moreau@esat.kuleuven.be](mailto:moreau@esat.kuleuven.be).

accurately represented on a coarser grid. The components of these eigenvectors are then eliminated on coarser grids [9, 23, 10]. The multilevel idea was also developed for the Fredholm integral equations and the resulting ill-posed problems [29]. The unregularized problem is solved by applying the Conjugate Gradient method (CG) for the normal equations on different levels. Regularization is applied by restricting the number of iterations on the different levels. In addition, principal eigenvectors can be used for preconditioning LSQR for ill-posed problems [28, 18]. For PDEs, multilevel preconditioning exploits the underlying idea that the operator is based on a discretized grid, often resulting in M-matrices. As for the Fredholm integral equations, the operator is based on a discretization of continuous functions on a grid. Data matrices do not have this property.

In machine learning, many linear systems of the form (1.1) have to be solved. Firstly, the regularization parameter  $\beta$  in (1.1) is often unknown and several values are tried in a cross-validation process. Secondly, different right-hand sides are often available or the linear system to be solved is part of a sampling algorithm. This means that even high computational costs for the construction of the preconditioner is often negligible compared to the many solves.

For applications from data science, state-of-the-art multilevel methods can not be used in their standard form. As opposed to grid based operators in PDEs, the matrices consist of samples and features and a hierarchy has to be designed on the data level. The resulting linear operator is a product of matrices and often dense. This means that the operator itself is not always available due to memory restrictions. There is no natural way to design the level hierarchy and the system matrix may not be available to design the coarse level directly from the operator. We thus propose to build a multilevel preconditioner based on the Multigrid idea by clustering the features of the data matrix, resulting in coarser levels. This can be done such that the principal eigenvectors are represented on the coarser levels. The number of required iterations is therefore reduced.

The paper is organized as follows. Section 2 describes different algorithms from machine learning and identifies the linear systems to be solved. Next, Section 3 describes a two-level preconditioner. Section 4 describes the framework for a multilevel hierarchy. In Section 5, the numerical results are presented. Section 6 tries to improve the two-level preconditioner by using the principal eigenvectors. Finally, Section 7 provides a discussion and conclusions are given in Section 8.

**2. Applications.** Data in machine learning consists of data samples and their features. Feature matrices can take any form, from dense or sparse and binary or real valued. The sample characteristics  $\mathbf{x}_i$  are collected in a feature matrix  $X \in \mathbb{R}^{N \times F}$  with  $N$  the number of samples or data points and  $F$  the number of features. Using the collected feature matrix, one tries to predict certain properties for new and unknown samples. These properties can be real valued and then the task at hand is regression or they can be limited to certain classes and then the task is classification. In this section, we will describe some techniques from machine learning where the linear system (1.1) is the main computational bottleneck, with  $\beta$  the regularization parameter. The techniques described here are mainly intended as illustrations and a comprehensive understanding is not required for the remaining sections. These applications require several linear systems with different right hand sides and justify the cost of more computational intensive preconditioners such as the preconditioner proposed in Section 3.

**2.1. Ridge Regression.** Suppose we have more samples than features and the result is an overdetermined system

$$X\mathbf{w} = \mathbf{b}$$

with  $\mathbf{b}$  the property of interest for the samples [3]. The ridge regression solution is determined by minimizing the squared error on  $\mathbf{b}$  ( $\mathbf{e} = X\mathbf{w} - \mathbf{b}$ ). Adding regularization to the solution vector  $\mathbf{w}$ , the optimization problem is given by

$$\min_{\mathbf{w}} \mathbf{e}^T \mathbf{e} + \beta \mathbf{w}^T \mathbf{w}$$

and the solution is

$$\mathbf{w} = (X^T X + \beta I)^{-1} X^T \mathbf{b}. \quad (2.1)$$

This technique is known in the field of numerical linear algebra as Tikhonov regularization for linear systems. The value of the regularization parameter  $\beta$  is unknown and several values are tried in a cross-validation process.

**2.2. Optimization by the Newton Method.** For certain optimization problems

$$\min_{\mathbf{w}} f(\mathbf{w})$$

the solution can be found by the Newton method which requires the inverse of the Hessian ( $\nabla^2 f(\mathbf{w})$ ). The Newton approach takes, at iteration  $k$ , the step  $\mathbf{s}_k = -(\nabla^2 f(\mathbf{w}_{k-1}))^{-1} \nabla f(\mathbf{w}_{k-1})$  and the iterative solution is updated as  $\mathbf{w}_k = \mathbf{w}_{k-1} + \mathbf{s}_k$  with  $\nabla f(\mathbf{w})$  the gradient. For large-scale data the inverse is not directly computed but a linear system is solved. Binary logistic regression [17] and L2 loss function Support Vector Machines [40] for example can be solved by the Newton Method and the linear systems are variants of (1.1) with the system matrix a product

$$\nabla^2 f(\mathbf{w}) = X^T D X + \beta I$$

where  $D$  is a diagonal matrix. More details can be found in the paper by Lin et al. [22] and the references therein.

**2.3. Matrix factorization.** Matrix factorization is a widely used technique in recommender systems. More generally, many machine learning problems can be formulated as a factorization of an incompletely filled matrix  $Y$ . Predicting the unknown values of this incomplete matrix is the objective of the task at hand. For example, the matrix in the Netflix challenge consists of user ratings for movies. The idea of matrix factorization is to determine a latent dimension  $D$  and factor matrices  $U, V$  such that  $Y = UV$  with  $Y \in \mathbb{R}^{R \times C}$ ,  $U \in \mathbb{R}^{R \times D}$  and  $V \in \mathbb{R}^{D \times C}$ . Bayesian Probabilistic Matrix Factorization (BPMF, [35]) assumes Gaussian noise on the observations and uses Markov Chain Monte Carlo. The BPMF model can be further extended by adding side information for the rows and/or columns of  $Y$ . Additional side information for movies is for example genre, director or actors. Simm et al. [36] describes a Gibbs sampling approach where a variant of the linear system (1.1)

$$(X^T X + \beta I)W = X^T(B + E_1) + E_2$$

has to be solved in each iteration with  $E_1$  and  $E_2$  noise matrices. Details can be found in [36] and the references there in.

**2.4. Linear discriminant analysis.** Dimension reduction techniques such as Principal Component Analysis (PCA) or Linear discriminant analysis (LDA) try to reduce the number of variables used in further analysis such as classification [3]. LDA is a supervised method that finds a linear mapping that maximally separates the classes while minimizing the within class variance. Defining the total-class-scatter matrix as  $S_T = X^T X$  and the between-class-scatter matrix as  $S_B$  the LDA optimization problem is

$$\max_{\mathbf{w} \in \mathbb{R}^N} \frac{\mathbf{w}^T S_B \mathbf{w}}{\mathbf{w}^T S_T \mathbf{w}}$$

and can be solved by finding the eigenvectors corresponding to the largest eigenvalues of

$$S_B \mathbf{w}_i = \lambda_i (S_T + \beta I) \mathbf{w}_i,$$

with  $\beta$  the regularization parameter. The low-rank and structure of the between-class-scatter matrix can be exploited and the main computational bottleneck is solving the linear system

$$(X^T X + \beta I) \mathbf{w} = X^T \mathbf{b} \quad (2.2)$$

with  $\mathbf{b}$  determined by the sample labels as detailed in [12].

**3. Two-level preconditioner.** The general idea of two-level preconditioning is to precondition a linear system from the solution of a linear system with less variables. This smaller linear system is obtained by projecting the large linear system on a subspace. Geometric Multigrid is used for the solution of elliptic partial differential equations. The discrete problem is solved hierarchically by approximating the original discretized PDE by coarser discretizations of the PDE [11]. The Multigrid principles were extended to Algebraic Multigrid using only the coefficients and sparsity pattern of the matrix instead of the geometry of the problem [31, 37, 41].

**3.1. The idea of two-level iterations.** The use of coarse grids for the solution of PDEs is motivated as follows. Many iterative schemes have poor convergence for PDEs. For a class of solvers, e.g. Gauss-Seidel iteration, the low frequency and near kernel components of the solution converge very slowly. These solvers are called smoothers because the remaining error of the solution is typically smooth. The coarse grids are used to remove the low frequency components of the error in a more efficient way. When the PDE is discretized on a coarse grid, the low frequency components of the solution on the fine grid and thus the error can be approximated well on to the coarse grid. Generally, a two-level solver consists of the following steps. A small number of iterations is performed on the fine level and a smooth error remains. The residual is mapped on the coarse level and this is called restriction. The restriction operator  $R$  maps a (long) vector on the fine grid to a (short) vector on the coarse grid. The linear system on the coarse grid is solved exactly. The coarse solution is mapped back to the fine grid using a prolongation operator  $P$ . This uses interpolation to identify all the unknowns on the fine grid and leads to a solution on the fine grid that mainly has high frequency components in the error. These components can then be further reduced by additional smoothing steps. There are several techniques to define  $R$  and  $P$  [37, 41, 5, 8].

For symmetric matrices, the restriction operator  $R$  is defined as the transpose of the interpolation operator  $P$ . Using the Galerkin approach the coarse level is defined by  $A_1 = P A_0 P^T$ . Assuming one step of Richardson's iteration as smoother [34], the resulting iteration matrix is

$$T = (I - \omega A_0)(I - P A_1^{-1} P^T A_0)(I - \omega A_0)$$

where the first factor is called post-smoothing, the third is pre-smoothing and the middle term is the coarse-grid correction. A more detailed explanation of (algebraic) Multigrid can be found in [41].

**3.2. Data matrices.** We want to adopt the idea of approximating error components on the coarse level and prolonging the coarse solution to the fine level. For matrices resulting from PDEs, the effect of aggregating elements is well known. In our case the matrix product of interest is  $X^T X$  with  $X$  a data matrix and this matrix product defines the covariance matrix.

The eigenvectors of the covariance matrix have a specific physical interpretation. A technique called Principal Component Analysis (PCA) finds the eigenvectors corresponding to the largest eigenvalues of the covariance matrix. PCA is in essence a projection that maximizes the total variance [3]. PCA actually finds the directions or principal components that projects the data on a subspace maximally preserving the variance of the data. Note that for applications the number of features is often higher than the number of samples, resulting in a large nullspace of  $X^T X$ . These eigenvectors are actually noise and contain no data information.

A widely used technique in machine learning is clustering. These clustering algorithms find subsets of similar samples or features based on a distance or similarity measure. Ideally, this results in subsets with small variance within one specific subset. Clustered subsets of features can be used to create aggregate features for the coarse level, preserving highest variance in the data set. Since highest variance is preserved in the coarse level, the principal components can be approximated on the coarse level.

Firstly, we propose to define an intuitive averaging restriction operator ( $\tilde{P}^T$ ) based on the clusters and this operator will be improved later. Specifically, a coarse feature  $\mathbf{c}_S$  consist of the average of the  $n_S$  features  $X(:, i)$  in one cluster  $S$  and  $i \in S$ :

$$\mathbf{c}_S = 1/n_S \sum_{i \in S} X(:, i).$$

The resulting restriction operator has the value  $1/n_S$  for each feature  $i \in S$  in the row corresponding to  $S$ . Assuming that the matrix  $X$  is ordered such that  $X = [X_1, X_2, \dots, X_{F_C}]$  with  $X_S$  the features belonging to cluster  $S = 1, \dots, F_C$  and  $F_C$  the coarse feature dimension, the restriction operator is

$$\tilde{P}^T = \begin{bmatrix} \overbrace{\frac{1}{n_1} \cdots \frac{1}{n_1}}^{n_1} & \overbrace{\frac{1}{n_2} \cdots \frac{1}{n_2}}^{n_2} & \cdots & \overbrace{\frac{1}{n_{F_C}} \cdots \frac{1}{n_{F_C}}}^{n_{F_C}} \\ & & \ddots & \\ & & & \end{bmatrix} \quad (3.1)$$

Note that the product is

$$\tilde{P}^T \tilde{P} = \begin{bmatrix} \frac{n_1}{n_1} & & & \\ & \frac{n_1}{n_2} & & \\ & & \ddots & \\ & & & \frac{n_{F_C}}{n_{F_C}} \end{bmatrix} \quad (3.2)$$

and thus  $\tilde{P}$  does not define a projection. The averaging interpolation operator can easily be adjusted such that the product  $P^T P$  is the identity matrix by defining the

coarse features as

$$\mathbf{c}_S = 1/\sqrt{n_S} \sum_{i \in S} X(:, i)$$

resulting in

$$P^T = \left[ \begin{array}{cccc} \overbrace{\frac{1}{\sqrt{n_1}} \cdots \frac{1}{\sqrt{n_1}}}^{n_1} & & & \\ & \overbrace{\frac{1}{\sqrt{n_2}} \cdots \frac{1}{\sqrt{n_2}}}^{n_2} & \cdots & \\ & & \ddots & \\ & & & \overbrace{\frac{1}{\sqrt{n_{F_C}}} \cdots \frac{1}{\sqrt{n_{F_C}}} }^{n_{F_C}} \end{array} \right] \quad (3.3)$$

Using the Galerkin approach [41] the coarse linear system becomes

$$\begin{aligned} P^T(X^T X + \beta I)P &= P^T X^T X P + P^T \beta I P \\ &= X_c^T X_c + \beta \underbrace{P^T P}_{=I} \end{aligned}$$

with  $X_c = XP$  the matrix with coarse features  $\mathbf{c}_S$  and the regularization parameter on the coarse level is equal to the regularization parameter on the fine level.

With the coarse level defined, we can create our two-level preconditioner. In AMG the coarse correction aims to eliminate the near kernel eigenvectors while the smoothing takes care of the eigenvectors associated with the large eigenvalues. In our approach, the problem is that both smoothing and coarse grid correction eliminate the error components of the principal eigenvectors. Therefore, smoothing does not have the same impact as for PDEs. We use one iteration of Richardson's iteration as post smoothing [34], resulting in the iteration matrix

$$T = \left( I - \omega(X^T X + \beta I) \right) \left( I - P(X_c^T X_c + \beta I_S)^{-1} P^T (X^T X + \beta I) \right). \quad (3.4)$$

The near kernel components are not present in the coarse level and are inefficiently solved by Richardson's iteration. Therefore, we propose to use our two-level preconditioner as an accelerator for Krylov subspace methods.

We adjust the notion of effective spectral radius as given by Notay [26] to describe the efficiency of the preconditioner.

**DEFINITION 3.1** (Effective spectral radius  $\rho_{\text{eff}}$ ). *We denote the effective spectral radius  $\rho_{\text{eff}}$  as the  $F_C$ th smallest eigenvalue of the iteration matrix*

$$T = \left( I - \omega(X^T X + \beta I) \right) \left( I - P(X_c^T X_c + \beta I_{F_C})^{-1} P^T (X^T X + \beta I) \right)$$

with  $F_C$  the column size of  $X_c$ .

This definition indicates how well the coarse level approximates a subset ( $F_C$ ) of the original spectrum. The remaining subset of the spectrum is eliminated by the Krylov subspace method on the fine level.

The coarse size  $F_C$  strongly influences the performance of the preconditioner. The spectrum can be divided in three parts: the noise components with small eigenvalues, the principal components represented in the coarse level and lastly the remaining components with eigenvalues in between the noise and the principal components. The coarse size determines the dimension of the principal components and the remaining

eigenvectors with nonzero eigenvalues. Depending on the required tolerance on the solution, these remaining components could cause slow convergence and are only eliminated on the fine level. If this happens, there is a possibility that the residual lies in the nullspace of the restriction operator  $P^T$  and the principal components are not present in the residual. Therefore, one smoothing iteration is required, since only applying the coarse correction would result in a zero solution and cause the fine level Krylov solver to break down.

**3.3. The ideal case.** In the ideal case, features within one cluster are identical. This means that the element values of the eigenvectors corresponding to the features within one cluster are equal. This additionally means that the eigenvector does not change within one cluster. This places a condition on our approach and the clustering algorithms should collect features in clusters such that the eigenvectors with large eigenvalues do not vary significantly within each cluster.

**DEFINITION 3.2** (Ideal data set for clustering). *The ideal data set for clustering  $X = [X_1, X_2, \dots, X_{F_C}]$  consists of sets of features  $X_i \in \mathbb{R}^{N \times n_i}$  consisting of  $n_i$  duplicate features  $\mathbf{x}_i$  for  $i = 1 \dots F_C$ .*

**THEOREM 3.3** (Ideal clustering case). *Let  $X$  satisfy Definition 3.2, the  $F_C$  eigenvectors with nonzero eigenvalues of  $X^T X$  are constant within the clusters. The prolongation operator  $P$  defined in (3.3) defines a projection  $PP^T$  for these eigenvectors and the eigenvectors of  $X^T X$  with nonzero eigenvalues have a one to one correspondence with the eigenvectors of  $P^T X^T X P$ .*

*Proof.* Given  $X = [X_1, X_2, \dots, X_{F_C}]$  the ideal data set with  $X_i$  consisting of  $n_i$  duplicate features  $\mathbf{x}_i$  for  $i = 1 \dots F_C$ . The matrix product  $X^T X$  has rank  $F_C$  and has the following block structure

$$X^T X = \begin{bmatrix} \mathbf{x}_1^T \mathbf{x}_1 \mathbb{1}^{n_1 \times n_1} & \mathbf{x}_1^T \mathbf{x}_2 \mathbb{1}^{n_1 \times n_2} & \dots & \mathbf{x}_1^T \mathbf{x}_{F_C} \mathbb{1}^{n_1 \times n_{F_C}} \\ \mathbf{x}_2^T \mathbf{x}_1 \mathbb{1}^{n_2 \times n_1} & \ddots & & \vdots \\ \vdots & & \ddots & \vdots \\ \mathbf{x}_{F_C}^T \mathbf{x}_1 \mathbb{1}^{n_{F_C} \times n_1} & \dots & & \mathbf{x}_{F_C}^T \mathbf{x}_{F_C} \mathbb{1}^{n_{F_C} \times n_{F_C}} \end{bmatrix}. \quad (3.5)$$

The matrix product  $X^T X$  can be written as

$$X^T X = PKP^T \quad (3.6)$$

with

$$K = \begin{bmatrix} \frac{\mathbf{x}_1^T \mathbf{x}_1}{n_1} & \frac{\mathbf{x}_1^T \mathbf{x}_2}{\sqrt{n_1} \sqrt{n_2}} & \dots & \frac{\mathbf{x}_1^T \mathbf{x}_{F_C}}{\sqrt{n_1} \sqrt{n_{F_C}}} \\ \frac{\mathbf{x}_2^T \mathbf{x}_1}{\sqrt{n_2} \sqrt{n_1}} & \ddots & & \vdots \\ \vdots & & \ddots & \vdots \\ \frac{\mathbf{x}_{F_C}^T \mathbf{x}_1}{\sqrt{n_{F_C}} \sqrt{n_1}} & \dots & & \frac{\mathbf{x}_{F_C}^T \mathbf{x}_{F_C}}{n_{F_C}} \end{bmatrix}. \quad (3.7)$$

Using the eigendecomposition of  $K = \hat{V} \Lambda \hat{V}^T$ , we have

$$X^T X = P \hat{V} \Lambda \hat{V}^T P^T. \quad (3.8)$$

By the structure of  $P$ , the eigenvectors with nonzero eigenvalues  $P \hat{\mathbf{v}}_i = \mathbf{v}_i$  are constant within each cluster. Given  $P \hat{\mathbf{v}}_i = \mathbf{v}_i$ , we have that  $PP^T \mathbf{v}_i = P \hat{\mathbf{v}}_i = \mathbf{v}_i$  and the interpolation operator (3.3) defines a projection for the eigenvectors with constant values within the clusters. Using the Rayleigh-Ritz method, the eigenpairs  $(\lambda_i, \hat{\mathbf{v}}_i)$  of  $P^T X^T X P$  can be used to find the original eigenpairs  $(\lambda_i, P \hat{\mathbf{v}}_i = \mathbf{v}_i)$ .  $\square$

**3.4. Clustering.** For matrices originating from grids, the coarser levels are defined by aggregating grid elements based on different criteria. Recall that for our applications, the matrix consists of samples with features. Similarity between features can be used to cluster these features. Typically a predefined distance measure  $d$  is used to define similarity, widely used distance measures are Euclidean distance, Jaccard distance and the cosine distance. All features within one cluster are then similar to each other and can be represented by the average feature. In this section we look at two clustering algorithms and one sub-sampling technique to create a coarser level.

**3.4.1. Leader clustering.** Leader-follower clustering is given in Algorithm 3.1 [16]. Starting from an initial set of leading clusters, each sample is added to an existing cluster if the sample is similar within the required tolerance to the cluster leader. This cluster leader can then optionally be updated. If a sample is not similar enough to any existing leader, it forms a new cluster.

---

**Algorithm 3.1** Leader-follower clustering

---

```

1: Initialise: given an initial set of clusters  $C$  and a distance measure  $d$ 
2: for each sample  $\mathbf{x}_i$  in  $X$  do
3:   index =  $\arg \min_{\mathbf{c}_s \in C} d(\mathbf{x}_i, \mathbf{c}_s)$ 
4:   if  $d(\mathbf{x}_i, \mathbf{c}_{\text{index}}) < \text{Tolerance}$  then
5:     Add  $\mathbf{x}_j$  to cluster  $\mathbf{c}_{\text{index}}$ 
6:     Optionally update cluster leader  $\mathbf{c}_{\text{index}} = \mathbf{c}_{\text{index}} + \frac{\mathbf{x}_j - \mathbf{c}_{\text{index}}}{n_{\text{index}}}$ 
7:   else
8:     Create new cluster based on  $\mathbf{x}_i$ 
9:   end if
10: end for

```

---

By varying the tolerance more or less clusters are found by leader-follower clustering. Small tolerance gives more clusters while high tolerance produces a smaller number of clusters. For our experiments we do not update the leader if a new sample is added to his followers. This is computationally more favorable during the setup phase of our multilevel preconditioner and preserves the leaders as original features.

**3.4.2. K-means++.** Another option to perform clustering on the features is K-means++. The algorithm exists of two phases [1]. During the setup phase, K-means++ finds initial  $K$  prototypes based on the distance between features. You may consider these prototypes as leaders for its cluster. The first prototype is chosen at random from the uniformly distributed features. The next initial prototype is randomly chosen with a probability weighted by the distance squared of each data points to the existing prototype.

The K-means algorithm then proceeds to the next phase by assigning each point to a cluster and then updating the prototypes according to its assigned cluster points. Once the prototypes are updated, the data points are reassigned. When the assignments no longer change, the algorithm has converged.

**3.4.3. Quadratic Rényi-entropy based subsampling.** Defining the coarser level can be done by maximizing the entropy of the coarser level or subset. Rényi-entropy [30, 15] based sub-sampling for large-scale data starts from a working set and a training set [4]. The entropy of the working set is the decisive parameter and the elements of the working set define the coarse level. Two random data points are chosen from both sets and the Rényi-entropy is calculated for both sets. The chosen



points from both sets are swapped and the Rényi-entropy is recalculated for both sets. If there is an increase in entropy for the working set, the data points are switched else the original sets are maintained.

The quadratic Rényi-entropy for a subset of size  $F_C$  is given by

$$S_{R2}^{F_C} = -\log \left( \frac{1}{F_C^2 |D|^2} \sum_{k=1}^{F_C} \sum_{l=1}^{F_C} \kappa \left( \frac{\mathbf{x}_k - \mathbf{x}_l}{D\sqrt{2}} \right) \right)$$

where  $\kappa$  is a kernel function and  $D$  the diagonal of the bandwidth values of the kernel in each dimension. Note that for each pair of data points under investigation the entropy can be updated based on both data points and there is no need to recalculate the entropy completely. These chosen features act then as the prototypes for the clusters and the remaining features are assigned to the cluster of the closest prototype.

**4. Multilevel preconditioning.** In AMG, coarsening is applied hierarchically until the size is sufficiently small and exact solvers can be applied. The multilevel concept has proven its merits in various applications [6]. The clustering algorithms are used hierarchically to create several levels of coarser features. For K-means and Rényi-entropy subsampling the size of the coarse level is chosen. For the leader follower algorithm, the threshold can be varied. The performance of the clusterings algorithms is determined by the correlation of the features. The smaller the dimension of the coarse level, the larger the variance within clusters.

---

**Algorithm 4.1** Flexible GMRES [32]      **Algorithm 4.2** Flexible CG [25]

---

```

1: Initialize:
    • Randomize  $\mathbf{x}_0$ 
    •  $\mathbf{r}_0 = \mathbf{b} - A\mathbf{x}_0$ 
    •  $\beta_0 = \|\mathbf{r}_0\|_2$ 
    •  $\mathbf{v}_1 = \mathbf{r}_0/\beta$ 
2: for  $j = 1, \dots, k$  do
3:    $\mathbf{z}_j = M_j^{-1}\mathbf{v}_j$ 
4:    $\mathbf{w} = A\mathbf{z}_j$ 
5:   for  $i = 1, \dots, i$  do
6:      $h_{i,j} = \langle \mathbf{w}, \mathbf{v}_i \rangle$ 
7:      $\mathbf{w} = \mathbf{w} - h_{i,j}\mathbf{v}_i$ 
8:   end for
9:    $h_{j+1,j} = \|\mathbf{w}\|_2$ 
10:   $\mathbf{v}_{j+1} = \mathbf{w}_{j+1,j}$ 
11: end for
12:  $\mathbf{y}_k = \arg \min_{\mathbf{y}} \|\beta \mathbf{e}_1 - H_k \mathbf{y}\|_2$ 
13:  $\mathbf{x}_k = \mathbf{x}_o + Z_k \mathbf{y}_k$ 

```

---

```

1: Given:  $m$ 
2: Initialize:
    •  $\mathbf{r}_0 = \mathbf{b}$ 
    •  $\mathbf{x}_0 = \mathbf{0}$ 
3: for  $i = 0, \dots, k$  do
4:    $\mathbf{z}_i = M_i^{-1}\mathbf{r}_i$ 
5:    $\mathbf{p}_i = \mathbf{z}_i - \sum_{k=i-m_i}^{i-1} \frac{\langle \mathbf{z}_i, A\mathbf{p}_k \rangle}{\langle \mathbf{p}_k, A\mathbf{p}_k \rangle} \mathbf{p}_k$ 
6:    $\mathbf{x}_{i+1} = \mathbf{x}_i + \frac{\langle \mathbf{p}_i, \mathbf{r}_i \rangle}{\langle \mathbf{p}_i, A\mathbf{p}_i \rangle} \mathbf{p}_i$ 
7:    $\mathbf{r}_{i+1} = \mathbf{r}_i - \frac{\langle \mathbf{p}_i, \mathbf{r}_i \rangle}{\langle \mathbf{p}_i, A\mathbf{p}_i \rangle} A\mathbf{p}_i$ 
8: end for
Advised truncation strategy:  $m_0 = 0$ ;
 $m_i = \max(1, \text{mod}(i, m+1))$  and  $m > 0, i > 0$ .

```

---

If the size of the coarse level remains large, iterative solvers should be used on that level. The use of iterative solvers on coarser levels as preconditioner for the finer levels requires flexible preconditioning. Flexible variants for GMRES and CG are available and given in respectively Algorithm 4.1 and Algorithm 4.2 [32, 25]. These flexible iterative solvers allow for the coarse level to be solved inexactly and hence even recursive multilevel Krylov-based cycles are possible [27]. A three-level

preconditioner could use flexible CG on the fine level preconditioned by CG on the medium level which in turn is preconditioned by a Cholesky decomposition on the coarsest level.

**5. Numerical Experiments.** We have applied multilevel preconditioning on the linear system

$$(X^T X + \beta I)\mathbf{x} = X^T \mathbf{b}$$

with  $\mathbf{b}$  a normal distributed random vector. The matrices  $X$  are chosen from the University of Florida sparse matrix collection [13] and from data sets from the UCI machine learning repository [20]. The characteristics of these matrices are summarized in Table 5.1. We assume here that many linear systems have to be solved, for example in the Gibbs sampler case for matrix factorization. Therefore, the setup cost of the multilevel preconditioner is not evaluated.

Data	Size	Nonzeros	Origin
lpsc105	105x163	340	Florida
trek10	104x478	8612	Florida
CNAE	1080x856	7233	UCI
micromass	360x1300	48713	UCI
DrivFace	606x6400	3878400 (dense)	UCI
air04	823x8904	72965	Florida
arcene	100x10000	540941	UCI

Table 5.1: The characteristics of the matrices in the experiments. We have tested our methods on actual data sets from the UCI machine learning repository [20] and matrices from the University of Florida sparse matrix collection [13].

The most general solver for the given applications is CG and the solution is computed within a certain tolerance ( $tol$ ) on the residual. We have applied FCG accelerated with a two-level preconditioner defined by the iteration matrix (3.4) and thus using one iteration of Richardson’s iteration with  $\omega = \frac{2}{\beta + \lambda_{\max}}$  as post-smoothing. The coarse level was solved exactly using the Cholesky decomposition, computed in advance. We solved each linear system 50 times and used the average execution time. Figure 5.1 shows the speed-up in function of the regularization parameter  $\beta$  of our preconditioner with respect to unpreconditioned CG with  $tol = 1e-6$ . The coarse level was created using leader-follower clustering and uses the modified average interpolation operator (3.3) to define the coarse level with the coarse size ( $F_C$ ) given within brackets. The experiments were executed using MATLAB R2017b<sup>1</sup>, on a computation server with Intel(R) Xeon(R) CPU E5-2697 v3 @ 2.60GHz and 125 GB of DRAM.

Figure 5.1 shows that the speed-up is dependent on the value of  $\beta$ . Larger  $\beta$ -values lead to smaller condition numbers and faster convergence for CG. Our two-level preconditioner achieves speed-up for most data sets for the full range of  $\beta$ -values and achieves speed-up for all data sets for small  $\beta$ -values. Speed-up was only achieved for the smaller regularization parameters for the *air04* matrix.

<sup>1</sup>The MATLAB code is available here: <https://people.cs.kuleuven.be/~joris.tavernier/>.

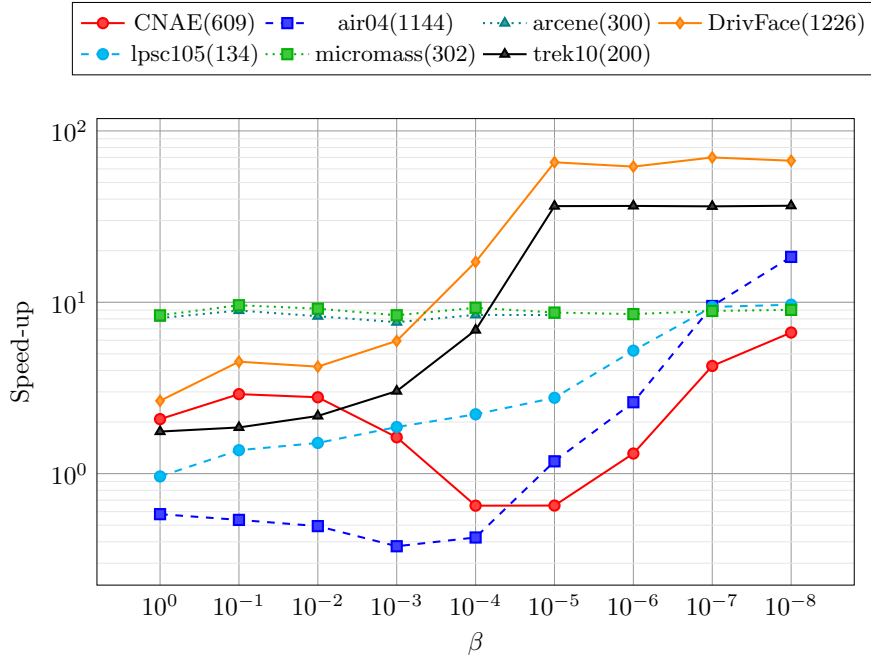


Fig. 5.1: The speed-up of FCG accelerated with our two-level preconditioner with respect to unpreconditioned CG in function of the regularization parameter  $\beta$  and tolerance =  $1e-6$  for all data sets except *micromass* for which the tolerance was  $1e-4$ . The feature size of the coarse level after Leader-follower clustering is given within brackets in the legend.

The performance of our preconditioner depends on both the regularization parameter and the required tolerance. Figure 5.2 shows the speed-up as a heatmap in function of the required tolerance and  $\beta$  for the data sets *trek10* and *DrivFace*. As can be seen from the figure, for large  $\beta$ -values and small tolerances speed-up was hard to achieve. Besides this specific setting, significant speed-up was generally achieved. For larger  $\beta$ -values, the system matrix is better conditioned and the original null space mapped to  $\beta$  gains in influence and is not well approximated on the coarse level. For small  $\beta$ -values, the nullspace is less influential on the fine level and the residual given to the coarse level contains less noise and the coarse level eliminates the residual more efficiently.

Figure 5.3 details the influence of the coarse level size for the *trek10* and *DrivFace* data sets. Increasing the size of the coarse level helps in achieving speed-up for larger values of  $\beta$ . For the smaller  $\beta$ -values the smaller coarse sizes result in larger speed-ups.

The only existing preconditioning technique directly applicable is Jacobi preconditioning [39, 14]. Figure 5.4 shows both the speed-up of our preconditioner and Jacobi preconditioning for *DrivFace*, *air04* and *trek10*. The figure shows that the speed-up of Jacobi preconditioning also depends on the  $\beta$ -value. Our preconditioner outperforms Jacobi preconditioning for almost all experiments.

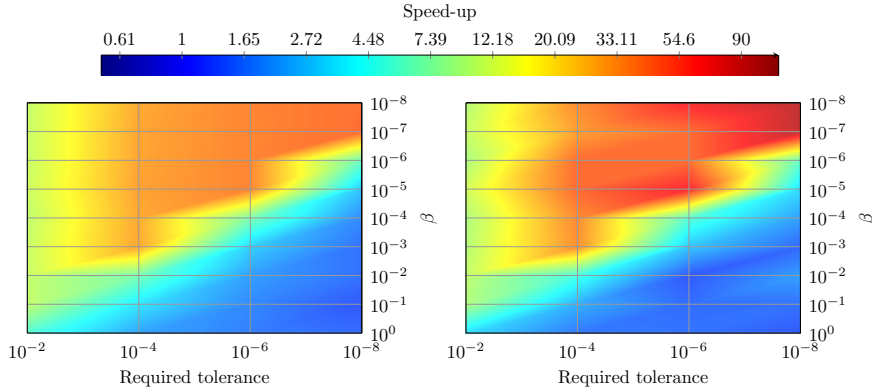


Fig. 5.2: The speed-up of FCG accelerated with our two-level preconditioner with respect to unpreconditioned CG for *trek10* with coarse size 200 (left) and *DrivFace* with coarse size 973 (right). The speed-up is given in function of the required tolerance and regularization parameter and is interpolated in between grid points.

**5.1. Choice of clustering algorithm.** The coarse level is created using clustering algorithms. In this section we investigate the influence of the clustering algorithm on the performance of the two-level preconditioner. In order to compare the different clustering algorithms, the coarse size was taken identically for all three algorithms. The coarse size created by Leader-follower clustering (LF) determined the value  $K$  in K-means++ (KM) and the working set in quadratic Rényi-entropy based subsampling (RE). We used the radial basis function kernel  $\kappa(\mathbf{x}_i - \mathbf{x}_j) = \exp\left(-\frac{\|\mathbf{x}_i - \mathbf{x}_j\|^2}{2\sigma^2}\right)$  to compute quadratic Rényi-entropy with  $\sigma = 0.6$ . Note that it is possible to fine tune the kernel for each data set specifically to improve the subset selection, but this was not done during the experiments.

The number of fine level CG and FCG iterations is given in Tables 5.2, 5.3, 5.4 and 5.5 along with the effective spectral radius ( $\rho_{\text{eff}}$ , Definition 3.1), the mean distance or dissimilarity within a cluster (Mean sim), the maximum distance within a cluster (Max sim) and the 75% similarity quantile (q75).

Table 5.2 shows the results for the *lpsc105* matrix. For KM and  $F_C = 56$  convergence was obtained for FCG in 308 iterations with  $m = 20$  (Algorithm 4.2). Using  $m = 40$ , convergence was obtained within 52 iterations. From the table, we can see that using LF clustering results in clusters with the smallest mean within-cluster-distance and in turn results in the minimum number of fine level iterations. Additionally, the preconditioner with the smallest  $\rho_{\text{eff}}$  results in the smallest number of fine level iterations.

The results for the *trek10* matrix are given in Table 5.3. KM resulted in the smallest within-cluster-distance and the lowest number of fine level iterations. As can be seen from the table, the smallest effective spectral radius is an indication of the performance. Note that for coarse size  $F_C = 120$  the smallest value of  $\rho_{\text{eff}}$  does not result in the smallest number of iterations but the differences in  $\rho_{\text{eff}}$  are small.

Using RE with our chosen kernel results in slow convergence for the *CNAE* data set, as shown in Table 5.4. This is reflected by a large value of  $\rho_{\text{eff}}$ . This may be due to our choice of kernel. LF clustering performs well for the *CNAE* data set and

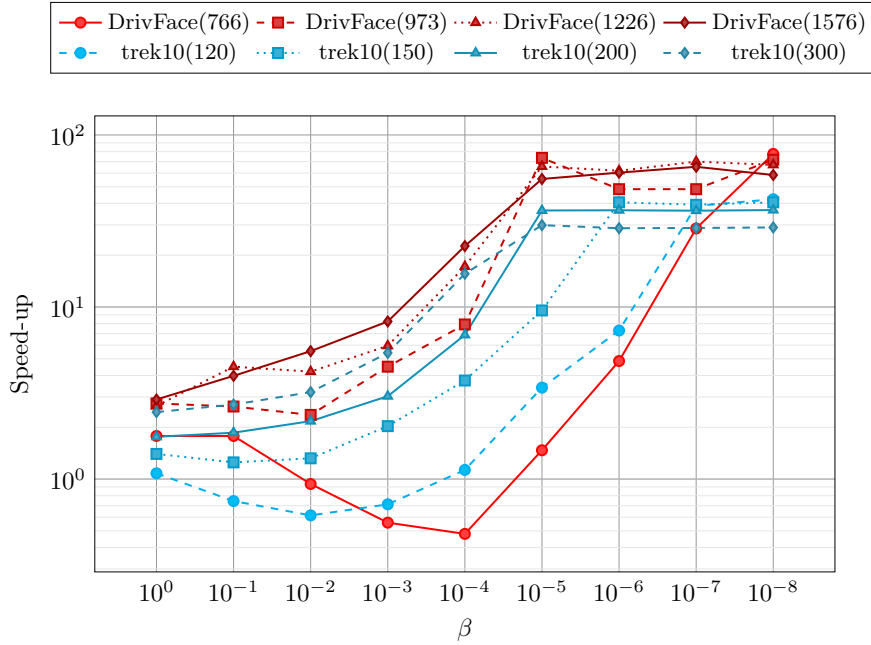


Fig. 5.3: The speed-up of FCG accelerated with our two-level preconditioner in comparison with unpreconditioned CG for tolerance = 1e-6. The results are shown for the two matrices *DrivFace* (red) and *trek10* (blue) and for different coarse sizes given within brackets in the legend.

Clustering algorithm	$\rho_{\text{eff}}$	$F_C$	CG	FCG	Mean sim	max sim	q75
LF	2.21e-13	56	66	<b>31</b>	1.60	2.45	1.73
RE	8.68e-13	56	66	35	1.70	2.94	2.00
KM	6.46e-11	56	66	52	1.97	3.32	2.24
LF	2.91e-14	90	66	<b>17</b>	1.32	2.00	1.41
RE	3.47e-11	90	66	20	1.53	2.87	2.00
KM	7.11e-11	90	66	58	1.77	2.94	2.05
LF	4.58e-13	104	66	<b>7</b>	1.31	1.41	1.41
RE	4.41e-10	104	66	12	1.44	2.49	1.73
KM	2.77e-10	104	66	10	1.63	2.94	2.05
LF	6.40e-10	134	66	<b>1</b>	0.26	1.00	1.00
RE	8.43e-10	134	66	3	0.95	2.24	1.41
KM	1.04e-09	134	66	3	0.93	2.49	2.00

Table 5.2: The number of fine level iterations for FCG, effective spectral radius ( $\rho_{\text{eff}}$ ), the mean similarity within a cluster (Mean sim), the maximum similarity within a cluster (Max sim) and the 75% similarity quantile (q75) for the three clustering algorithms with  $\beta = 1e-6$  and  $tol = 1e-6$  for different coarse sizes ( $F_C$ ) and the *lpsc105* data set. The number of fine level iterations of (unpreconditioned) CG are given for comparison. For KM and  $F_C = 56$ , the value of  $m = 40$  in FCG was used instead of  $m = 20$ .

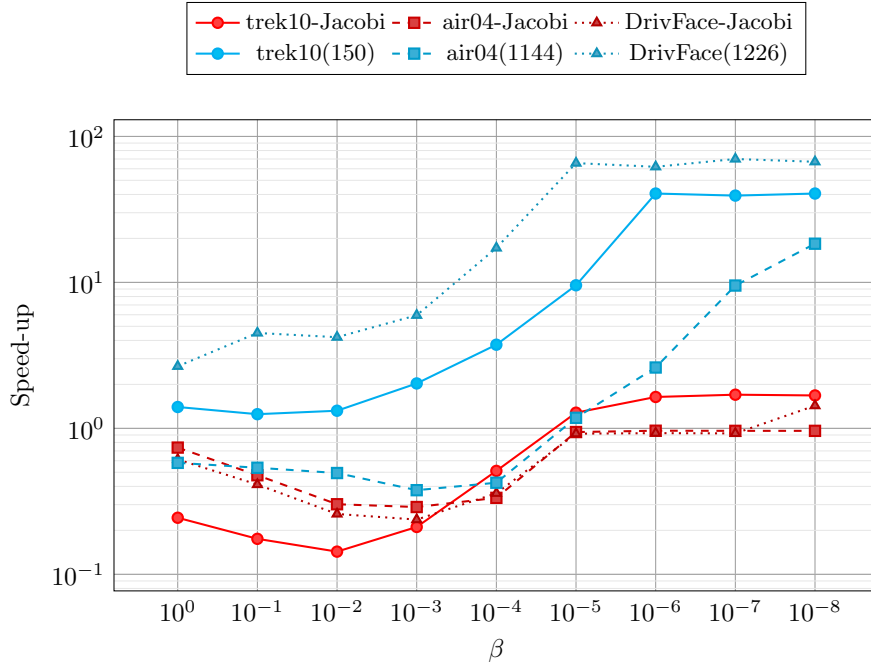


Fig. 5.4: The speed-up of FCG accelerated with our two-level preconditioner (blue) in comparison with unpreconditioned CG and the speed-up of diagonally preconditioned CG (Jacobi, red) in comparison with unpreconditioned CG using a tolerance of  $1e-6$  for the *DrivFace*, *air04* and *trek10* matrices.

outperforms KM for all coarse sizes. Note that there is perfect clustering for  $F_C = 664$ . This happens because there are redundant features in the data set. KM does not find this perfect clustering due to the averaging of the features in each update step.

Table 5.5 shows that for the *air04* matrix, using RE leads to less fine level iterations for the small coarse sizes. For large coarse levels, KM results in the smallest number of fine level iterations.

The choice of clustering algorithm strongly depends on the data set. Here we used three different clustering algorithms to create the coarse level. It is possible to use hierarchical clustering algorithms to create the different levels. These clustering algorithms depend on a chosen similarity measure. Using specific data dependent similarity measures may improve the resulting clustering.

**5.2. Three level preconditioner.** We have experimented with a three level preconditioner to accelerate FCG by applying FCG on the middle level accelerated with a two-level preconditioner using Cholesky decomposition on the coarsest level. We used the same setup as before with only one iteration of Richardson’s iteration as post-smoothing. Table 5.6 shows the size of the middle and coarse level along with the number of fine level and middle level number of iterations with the tolerance for FCG set to  $1e-6$  for both the fine and middle level. The speed-up is given with respect to (unpreconditioned) CG and the number of fine level iterations using FCG accelerated with a two-level preconditioner for both the coarse and middle level are given for comparison.

Clustering algorithm	$\rho_{\text{eff}}$	$F_C$	CG	FCG	Mean similarity	Max similarity	q75
LF	3.96e-11	60	248	353	13.2	32.3	17.0
RE	1.02e-11	60	248	291	8.21	90.0	10.0
KM	5.71e-13	60	248	<b>69</b>	7.61	49.3	8.83
LF	3.27e-10	80	248	74	12.1	28.3	15.7
RE	1.67e-12	80	248	43	7.91	126	8.31
KM	2.68e-12	80	248	<b>38</b>	7.21	53.7	8.37
LF	4.51e-07	120	248	7	10.0	22.2	12.8
RE	3.50e-07	120	248	3	6.83	61.2	7.14
KM	4.97e-07	120	248	<b>1</b>	6.39	42.1	7.81
LF	2.97e-06	150	248	1	9.07	18.0	11.4
RE	6.57e-07	150	248	1	6.95	72.5	7.42
KM	8.25e-07	150	248	1	5.83	40.6	7.14

Table 5.3: The effective spectral radius ( $\rho_{\text{eff}}$ ), number of fine level FCG iterations, the mean similarity within a cluster, the maximum similarity within a cluster and the 75% similarity quantile (q75) for the three clustering algorithms with  $\beta = 1\text{e-}6$  and  $\text{tol} = 1\text{e-}6$  for different coarse sizes ( $F_C$ ) and the *trek10* data set.

Clustering algorithm	$\rho_{\text{eff}}$	$F_C$	CG	FCG	Mean similarity	Max similarity	q75
LF	1.04e-12	335	631	<b>108</b>	1.55	2.45	1.73
RE	9.85e-01	335	631	199	1.65	11.2	1.73
KM	1.38e-12	335	631	177	1.66	8.25	1.73
LF	1.75e-12	418	631	<b>81</b>	1.39	2.00	1.41
RE	9.95e-01	418	631	667	1.61	14.0	1.73
KM	2.96e-10	418	631	242	1.62	5.83	1.73
LF	5.67e-10	609	631	<b>83</b>	0.22	1.41	0.00
RE	9.99e-01	609	631	157	1.14	4.24	1.41
KM	2.72e-09	609	631	164	0.68	2.45	1.41
LF	4.19e-10	664	631	<b>1</b>	0.00	0.00	0.00
RE	9.99e-01	664	631	183	0.99	3.32	1.41
KM	2.19e-09	664	631	20	0.13	2.00	0.00

Table 5.4: The number of fine level FCG iterations, effective spectral radius ( $\rho_{\text{eff}}$ ), the mean similarity within a cluster, the maximum similarity within a cluster and the 75% similarity quantile (q75) for the three clustering algorithms varying the coarse size ( $F_C$ ) with  $\beta = 1\text{e-}6$  and  $\text{tol} = 1\text{e-}6$  for the *CNAE* data set.

As can be seen from Table 5.6, speed-up is achieved using FCG recursively on two levels. If the size of the coarse levels is chosen too small, no speed-up was achieved. Choosing the correct size for the different levels is important. Depending on the characteristics of the data, clustering too aggressively and reducing the number of features drastically may result in slow convergence.

**5.3. Large-scale.** We have applied our two-level preconditioner on a larger data set from chemogenomics called ChEMBL described in [36]. The data set consist of 167668 samples with 291714 features. The matrix is sparse and has 12246376 nonzero elements. Using Leader-follower clustering with a threshold of  $1\text{e-}4$  a coarse level was created with a data matrix consisting of 179745 features with 11322834 nonzero elements. The two-level preconditioner was implemented in C++ and compiled with

Clustering algorithm	$\rho_{\text{eff}}$	$F_C$	CG	FCG	Mean similarity	Max similarity	q75
LF	1.23e-07	906	324	31	2.73	4.24	3.16
RE	1.03e-07	906	324	<b>16</b>	2.81	5.00	3.32
KM	9.52e-08	906	324	21	2.50	4.24	3.00
LF	1.50e-07	1144	324	13	2.64	4.00	3.16
RE	1.14e-07	1144	324	<b>6</b>	2.77	4.58	3.32
KM	1.37e-07	1144	324	11	2.40	4.36	2.83
LF	1.69e-07	1833	324	13	2.60	3.74	2.83
RE	2.20e-07	1833	324	7	2.62	4.58	3.16
KM	2.13e-07	1833	324	<b>4</b>	2.14	4.24	2.83
LF	1.68e-07	2185	324	7	2.42	3.46	2.83
RE	1.82e-07	2185	324	5	2.45	4.47	3.16
KM	1.79e-07	2185	324	<b>2</b>	2.01	4.12	2.65

Table 5.5: The number of fine level FCG iterations, effective spectral radius ( $\rho_{\text{eff}}$ ), the mean similarity within a cluster, the maximum similarity within a cluster and the 75% similarity quantile (q75) for the three clustering algorithms and varying coarse size ( $F_C$ ) with  $\beta = 1e-6$  and  $tol = 1e-6$  for the *air04* data set.

Data	[Middle level, Coarse level]	(Fine)[Middle] level iterations	Speed-up vs CG	Two-level middle iterations	Two-level coarse iterations
trek10	[150, 120]	(1)[1]	8.04	1	7
trek10	[150, 100]	(3)[13,32,1]	0.876	1	14
trek10	[120, 100]	(3)[10,24,1]	1.37	1	14
trek10	[120, 80]	(3)[36,44,1]	0.61	1	38
DrivFace	[1576, 973]	(1)[1]	27.47	1	1
DrivFace	[1226, 766]	(1)[1]	59.57	1	1
DrivFace	[766, 613]	(2)[8,38]	9.92	1	20
DrivFace	[613, 484]	(58)[409,1371,22,...]	0.05	20	28
air04	[3115, 1833]	(1)[1]	4.40	1	4
air04	[2185, 1833]	(4)[16,12,23,3]	0.32	2	4
air04	[2185, 1144]	(4)[10,70,36,70]	0.25	2	11

Table 5.6: Experiments with a three-level preconditioner with FCG on the fine and middle level. The number of iterations are shown for  $\beta = 1e-6$  and  $tol = 1e-6$  on the fine level and the middle level. Speed-up is given with respect to (unpreconditioned) CG. The number of fine level iterations are given for FCG accelerated with a two-level preconditioner with the coarse size equal to the middle and coarse level of the three-level.

GCC version 7.2.0 and compile optimizations were used. CG was used to solve the coarse linear systems inexactly up to a certain tolerance.

Table 5.7 shows the speed-up of our two-level preconditioner with respect to unpreconditioned CG. The fine level tolerance was set to  $1e-6$  for FGMRES and FCG. From Table 5.7 we can see that depending on the coarse level tolerance we only need one or two fine level iterations. The coarse level system is solved iteratively and remains ill-conditioned. The speed-up results partly from the reduction of number of nonzeros in the data matrix. The solution of the coarse level is sufficient to find the solution on the fine level within the required tolerance. The speed-up results partly



Fine level Solver	Coarse tolerance	$\beta$	Fine level Iterations	Time CG (s)	Speed-up
FCG	1.00e-03	1.00e-02	2	1379.13	1.17
FCG	1.00e-03	1.00e-04	2	6271.74	1.13
FCG	1.00e-03	1.00e-06	2	7347.01	1.17
FCG	1.00e-03	1.00e-08	2	7408.58	1.15
FCG	1.00e-06	1.00e-02	1	1412.56	1.20
FCG	1.00e-06	1.00e-04	1	6354.13	1.16
FCG	1.00e-06	1.00e-06	1	7519.23	1.18
FCG	1.00e-06	1.00e-08	1	7504.82	1.18
FGMRES	1.00e-06	1.00e-02	1	1386.59	1.16
FGMRES	1.00e-06	1.00e-04	1	6292.82	1.20
FGMRES	1.00e-06	1.00e-06	1	7456.53	1.31
FGMRES	1.00e-06	1.00e-08	1	7325.92	1.32

Table 5.7: Result for two-level preconditioner for the ChEMBL data with inexact coarse solves. The tolerance on the fine level was set to 1e-6 with equal  $\beta$  on both levels. The number of fine level iterations and speed-up with respect to (unpreconditioned) CG are given for FCG or FGMRES accelerated with our two-level preconditioner.

from the reduction in nonzero elements on the coarse level, the number of nonzeros is reduced by a factor 1.08.

**6. Least-squares interpolation.** An alternative for the prolongation operation for PDEs is to define the interpolation operator to exactly interpolate certain prototype vectors in a least-squares manner and is used in Bootstrap AMG [7, 24]. We assume that the coarse level approximates the principal components reasonably well and suppose the  $K$  first principal components  $V = \{\mathbf{v}_1, \dots, \mathbf{v}_K\}$  and  $V \in \mathbb{R}^{F \times K}$  are given. Least squares interpolation adjusted for our application minimizes the error squared for each feature  $i$  and thus each row  $P(i, :)$  for these principal components  $V$

$$P(i, :) = \arg \min_{p_{ij}, j \in \mathcal{C}_i} \sum_{k=1}^K \eta_k \left( \mathbf{v}_k(i) - \sum_{j \in \mathcal{C}_i} p_{ij} \mathbf{v}_k(j) \right)^2 \quad (6.1)$$

with  $\mathcal{C}_i$  the coarse features used to interpolate the value of feature  $i$  and weights  $\eta_k = \langle (X^T X + \beta I) \mathbf{v}_k, \mathbf{v}_k \rangle$  chosen to reflect the energy norm. For example, the  $k$ -closest leaders to feature  $i$  of leader-follower clustering can be chosen as the coarse features used in the interpolation process. The original least squares interpolation was extended to include the residuals  $\mathbf{r}_k = (X^T X + \beta I) \mathbf{v}_k$  for  $k = 1, \dots, K$  as detailed in [7, 24]. The optimization problem (6.1) changes to

$$P(i, :) = \arg \min_{p_{ij}, j \in \mathcal{C}_i} \sum_{k=1}^K \eta_k \left( \left( 1 - \frac{\lambda_k}{X_{(:,i)}^T X_{(:,i)} + \beta} \right) \mathbf{v}_k(i) - \sum_{j \in \mathcal{C}_i} p_{ij} \mathbf{v}_k(j) \right)^2 \quad (6.2)$$

and incorporates the residual  $\mathbf{r}_k = (X^T X + \beta I) \mathbf{v}_k$  divided by the diagonal of  $X^T X + \beta I$  with  $\mathbf{v}_k$  an eigenvector and hence  $\mathbf{r}_k(i) = \lambda_k \mathbf{v}_k(i)$ . This means that the largest eigenvalues influence the minimization process stronger than the smaller ones.

We calculated the eigenvectors with the largest eigenvalues and tried to improve the interpolation by exactly interpolating these eigenvectors from the coarse level.

Tables 6.1 and 6.2 show fine level iterations for 16 and 32 eigenvectors with 1 or 2 coarse features used for interpolation ( $\mathcal{C}_i$ ) in (6.1, 6.2) for respectively the *trek10* matrix and the *DrivFace* data set. As can be seen from Table 6.1, for the smallest coarse level ( $F_C = 60$ ) the number of fine level iterations were reduced by exactly interpolating the eigenvectors for the *trek10* matrix. Note that  $\rho_{\text{eff}}$  is an indication for the efficiency but the number of fine level iterations is not always explained by this value. For larger coarse levels, using the adjusted average (3.3) resulted in the smallest number of fine level iterations.

Interpolation operator	$\rho_{\text{eff}}$	$F_C$	CG	FCG	Coarse interpolating features	number of eigenvectors
adjusted average (3.3)	3.96e-11	60	248	353	1	0
least squares a (6.1)	8.00e-02	60	248	187	1	16
least squares a (6.1)	7.69e-06	60	248	192	2	16
least squares a (6.1)	3.91e-12	60	248	274	1	32
least squares a (6.1)	2.77e-02	60	248	237	2	32
least squares b (6.2)	4.73e-12	60	248	243	1	16
least squares b (6.2)	2.03e-01	60	248	162	2	16
least squares b (6.2)	2.87e-11	60	248	181	1	32
least squares b (6.2)	9.47e-02	60	248	<b>153</b>	2	32
adjusted average (3.3)	3.27e-10	80	248	<b>74</b>	1	0
least squares a (6.1)	4.36e-10	80	248	172	1	16
least squares a (6.1)	6.46e-01	80	248	94	2	16
least squares a (6.1)	6.81e-11	80	248	128	1	32
least squares a (6.1)	1.87e-02	80	248	136	2	32
least squares b (6.2)	1.28e-11	80	248	79	1	16
least squares b (6.2)	2.22e-02	80	248	380	2	16
least squares b (6.2)	4.92e-11	80	248	78	1	32
least squares b (6.2)	6.39e-01	80	248	153	2	32
adjusted average (3.3)	4.51e-07	120	248	<b>7</b>	1	0
least squares a (6.1)	1.02e-06	120	248	<b>7</b>	1	16
least squares a (6.1)	1.00e+00	120	248	11	2	16
least squares a (6.1)	9.38e-07	120	248	<b>7</b>	1	32
least squares a (6.1)	9.99e-01	120	248	13	2	32
least squares b (6.2)	6.93e-07	120	248	9	1	16
least squares b (6.2)	1.00e+00	120	248	14	2	16
least squares b (6.2)	1.17e-06	120	248	<b>7</b>	1	32
least squares b (6.2)	1.00e+00	120	248	13	2	32
adjusted average (3.3)	2.97e-06	150	248	1	1	0
least squares a (6.1)	1.35e-06	150	248	1	1	16
least squares a (6.1)	1.00e+00	150	248	1	2	16
least squares a (6.1)	1.20e-06	150	248	1	1	32
least squares a (6.1)	1.00e+00	150	248	1	2	32
least squares b (6.2)	4.04e-06	150	248	1	1	16
least squares b (6.2)	1.00e+00	150	248	1	2	16
least squares b (6.2)	3.80e-06	150	248	1	1	32
least squares b (6.2)	1.00e+00	150	248	1	2	32

Table 6.1: The number of fine level FCG iterations accelerated with a two-level preconditioner for different interpolation operators  $P$  for the *trek10* data set. The number of coarse interpolation features ( $\mathcal{C}_i$ ) and the number of principal eigenvectors for the least-squares interpolation operators are varied. The number of (unpreconditioned) CG iterations are given for comparison.

For the *DrivFace* data set, using the least-squares interpolation results in small improvements in fine level iterations with respect to the adjusted averaging interpolation, as shown in Table 6.2. Using more coarse features in the interpolation process was not beneficial for the performance.

Interpolation operator	$\rho_{\text{eff}}$	$F_C$	CG	FCG	Coarse interpolating features	number of eigenvectors
adjusted average (3.3)	4.44e-11	308	426	61	1	$\emptyset$
least squares a (6.1)	4.99e-11	308	426	<b>60</b>	1	16
least squares a (6.1)	1.05e-04	308	426	84	2	16
least squares a (6.1)	3.41e-11	308	426	<b>60</b>	1	32
least squares a (6.1)	5.77e-05	308	426	80	2	32
least squares b (6.2)	5.68e-11	308	426	<b>60</b>	1	16
least squares b (6.2)	8.92e-05	308	426	87	2	16
least squares b (6.2)	3.73e-11	308	426	<b>60</b>	1	32
least squares b (6.2)	6.45e-05	308	426	86	2	32
adjusted average (3.3)	2.59e-10	484	426	30	1	$\emptyset$
least squares a (6.1)	2.56e-10	484	426	<b>29</b>	1	16
least squares a (6.1)	1.07e-03	484	426	44	2	16
least squares a (6.1)	2.15e-10	484	426	<b>29</b>	1	32
least squares a (6.1)	2.03e-04	484	426	40	2	32
least squares b (6.2)	2.35e-10	484	426	<b>29</b>	1	16
least squares b (6.2)	6.09e-04	484	426	44	2	16
least squares b (6.2)	2.44e-10	484	426	<b>29</b>	1	32
least squares b (6.2)	2.93e-04	484	426	41	2	32
adjusted average (3.3)	4.03e-06	613	426	19	1	$\emptyset$
least squares a (6.1)	1.90e-06	613	426	<b>15</b>	1	16
least squares a (6.1)	8.18e-01	613	426	42	2	16
least squares a (6.1)	4.19e-06	613	426	<b>15</b>	1	32
least squares a (6.1)	5.46e-01	613	426	36	2	32
least squares b (6.2)	2.54e-06	613	426	17	1	16
least squares b (6.2)	8.34e-01	613	426	51	2	16
least squares b (6.2)	2.47e-06	613	426	17	1	32
least squares b (6.2)	7.63e-01	613	426	44	2	32

Table 6.2: The effective spectral radius ( $\rho_{\text{eff}}$ ) and number of fine level FCG iterations. Different interpolation operators  $P$  are used to accelerate FCG with a two-level preconditioner for the *DrivFace* data set. The number of coarse interpolation features ( $C_i$ ) and the number of principal eigenvectors for the least-squares interpolation operators are varied. The number of (unpreconditioned) CG iterations are given for comparison.

**7. Discussion.** The performance of our presented preconditioner depends on several factors. Firstly, the efficiency of our preconditioner is data dependent. Clustering algorithms perform differently for distinct data sets. It may very well be that one clustering algorithm does not lead to speed-up while another clustering does. We detailed the performance of the two-level preconditioner and have shown results for a three-level preconditioner. Choosing hierarchical clustering algorithms can result in a better coarse level hierarchy than reapplying the same clustering algorithm on each level. Note that different clustering algorithms might lead to different densities of the sparse matrices. For very sparse data, it may be that clustering the features does not significantly reduce the number of nonzeros on the coarse level. Hence, the amount of work required by a Krylov solver on the coarse level might not differ too much with the fine level.

Using the flexible variant of CG or GMRES allows to use (F)CG or (F)GMRES on the coarser levels and allows for inexact solves on the coarse level. The regularization parameter determines the condition number of the linear system to be solved. Ideally the regularization parameter on the coarse level is equal to the fine level, but it may be that choosing a larger regularization parameter on the coarse level results in faster convergence. By choosing a larger regularization parameter on the coarse level, the

condition number of the linear system on the coarse level reduces and the number of iterations generally decreases. If the number of fine level iterations does not increase, further speed-up is achieved.

We investigated clustering in the column space (features) of  $X$ . It is also possible to additionally cluster in the row space (samples) leading to a coarse matrix with even less nonzeros. This means that the work on the coarse level is reduced, but clustering both the features and samples generally results in additional fine level iterations. This is a trade-off between work on the coarse level and additional computational work on the fine level.

Generally the performance depends on numerous factors. We do not recommend our approach when only one linear system has to be solved. Finding the right hierarchy of levels and choosing the clustering algorithm requires some fine tuning. Therefore, we suggest that our preconditioner is only considered when many linear systems have to be solved. This is, for example, the case for different regularization parameters or several right-hand sides. Creating the preconditioner requires preprocessing, but significant speed-up is likely to be achieved. For very sparse and binary data matrices, large regularization and small tolerance, speed-up is unlikely to be achieved. For data with highly correlated sets of features, our preconditioner will likely achieve speed-up.

There are numerous ways to design our proposed preconditioner. Initially, we propose to start from a two-level preconditioner. Creating a coarse level requires a clustering algorithm. The performance of clustering algorithms is data dependent. If a certain class of clustering algorithms for your specific data set works well, it is likely that the resulting clusters can be used for our preconditioner. Otherwise K-means generally works well for a variety of data sets. Next, the coarse size should be chosen in function of the specific range of regularization values as illustrated in Figure 5.3. Achieving speed-up with large regularization will require a larger coarse level than for small regularization. If a subset of the principal components is available, the number of fine level iterations could be further reduced by using least-squares interpolation (6.1). A well performing two-level preconditioner can then be extended to a multilevel preconditioner recursively or by using hierarchical clustering algorithms.

**8. Conclusion.** The multilevel preconditioner described here finds its application in machine learning. We have shown that it is possible to approximate the principal eigenvectors on a coarser level by means of clustering the columns of the feature matrix. Using this preconditioner to accelerate FCG, speed-up was achieved for almost all data sets. A speed-up of 100 was observed for the dense *DriveFace* matrix for a specific preconditioning setting. The efficiency of the preconditioner was shown to be data dependent. Furthermore, it was illustrated that the choice of the regularization parameter plays an important role and our proposed multilevel preconditioner is less effective for high regularization.

**9. Acknowledgements.** This work was supported Research Foundation - Flanders (FWO, No. G079016N).

#### REFERENCES

- [1] D. ARTHUR AND S. VASSILVITSKII, *k-means++: The advantages of careful seeding*, in Proceedings of the eighteenth annual ACM-SIAM symposium on Discrete algorithms, Society for Industrial and Applied Mathematics, 2007, pp. 1027–1035.
- [2] M. BENZI, C. D. MEYER, AND M. TUMA, *A sparse approximate inverse preconditioner for the conjugate gradient method*, SIAM Journal on Scientific Computing, 17 (1996),

- pp. 1135–1149, <https://doi.org/10.1137/S1064827594271421>, <https://doi.org/10.1137/S1064827594271421>, <https://arxiv.org/abs/https://doi.org/10.1137/S1064827594271421>.
- [3] C. M. BISHOP, *Pattern Recognition and Machine Learning*, Springer-Verlag New York, 2006.
  - [4] K. D. BRABANTER, J. D. BRABANTER, J. SUYKENS, AND B. D. MOOR, *Optimized fixed-size kernel models for large data sets*, Computational Statistics & Data Analysis, 54 (2010), pp. 1484 – 1504, <https://doi.org/https://doi.org/10.1016/j.csda.2010.01.024>, <http://www.sciencedirect.com/science/article/pii/S0167947310000393>.
  - [5] A. BRANDT, *General highly accurate algebraic coarsening*, Electronic Transactions on Numerical Analysis, 10 (2000), pp. 1–20.
  - [6] A. BRANDT, *Multiscale scientific computation: Review 2001*, in Multiscale and Multiresolution Methods, T. J. Barth, T. Chan, and R. Haines, eds., Berlin, Heidelberg, 2002, Springer Berlin Heidelberg, pp. 3–95.
  - [7] A. BRANDT, J. BRANNICK, K. KAHL, AND I. LIVSHITS, *Bootstrap AMG*, SIAM Journal on Scientific Computing, 33 (2011), pp. 612–632, <https://doi.org/10.1137/090752973>, <https://arxiv.org/abs/https://doi.org/10.1137/090752973>.
  - [8] J. J. BRANNICK AND R. D. FALGOUT, *Compatible relaxation and coarsening in algebraic multigrid*, SIAM Journal on Scientific Computing, 32 (2010), pp. 1393–1416, <https://doi.org/10.1137/090772216>, <https://arxiv.org/abs/https://doi.org/10.1137/090772216>.
  - [9] M. BREZINA, R. FALGOUT, S. MACLACHLAN, T. MANTEUFFEL, S. MCCORMICK, AND J. RUGE, *Adaptive smoothed aggregation (asa) multigrid*, SIAM Review, 47 (2005), pp. 317–346, <https://doi.org/10.1137/050626272>, <https://doi.org/10.1137/050626272>, <https://arxiv.org/abs/https://doi.org/10.1137/050626272>.
  - [10] M. BREZINA, R. FALGOUT, S. MACLACHLAN, T. MANTEUFFEL, S. MCCORMICK, AND J. RUGE, *Adaptive algebraic multigrid*, SIAM Journal on Scientific Computing, 27 (2006), pp. 1261–1286, <https://doi.org/10.1137/040614402>, <https://doi.org/10.1137/040614402>, <https://arxiv.org/abs/https://doi.org/10.1137/040614402>.
  - [11] W. BRIGGS, V. HENSON, AND S. MCCORMICK, *A Multigrid Tutorial, Second Edition*, Society for Industrial and Applied Mathematics, second ed., 2000, <https://doi.org/10.1137/1.9780898719505>, <https://epubs.siam.org/doi/abs/10.1137/1.9780898719505>, <https://arxiv.org/abs/https://epubs.siam.org/doi/pdf/10.1137/1.9780898719505>.
  - [12] D. CAI, X. HE, AND J. HAN, *Srda: An efficient algorithm for large-scale discriminant analysis*, IEEE Transactions on Knowledge and Data Engineering, 20 (2008), pp. 1–12.
  - [13] T. A. DAVIS AND Y. HU, *The university of florida sparse matrix collection*, ACM Transactions on Mathematical Software (TOMS), 38 (2011), p. 1.
  - [14] J. DEMMEL, *Applied Numerical Linear Algebra*, Society for Industrial and Applied Mathematics, 1997.
  - [15] M. GIROLAMI, *Orthogonal series density estimation and the kernel eigenvalue problem*, Neural Computation, 14 (2002), pp. 669–688, <https://doi.org/10.1162/089976602317250942>, <https://doi.org/10.1162/089976602317250942>, <https://arxiv.org/abs/https://doi.org/10.1162/089976602317250942>.
  - [16] J. A. HARTIGAN, *Clustering Algorithms*, John Wiley & Sons, Inc., New York, NY, USA, 99th ed., 1975.
  - [17] D. W. HOSMER JR, S. LEMESHOW, AND R. X. STURDIVANT, *Applied logistic regression*, vol. 398, John Wiley & Sons, 2013, <https://doi.org/10.1002/0471722146>.
  - [18] M. JACOBSEN, P. C. HANSEN, AND M. A. SAUNDERS, *Subspace preconditioned lsqr for discrete ill-posed problems*, BIT Numerical Mathematics, 43 (2003), pp. 975–989, <https://doi.org/10.1023/B:BITN.0000014547.88978.05>, <https://doi.org/10.1023/B:BITN.0000014547.88978.05>.
  - [19] D. S. KERSHAW, *The incomplete cholesky–conjugate gradient method for the iterative solution of systems of linear equations*, Journal of Computational Physics, 26 (1978), pp. 43 – 65, [https://doi.org/https://doi.org/10.1016/0021-9991\(78\)90098-0](https://doi.org/https://doi.org/10.1016/0021-9991(78)90098-0), <http://www.sciencedirect.com/science/article/pii/0021999178900980>.
  - [20] M. LICHMAN, *UCI machine learning repository*, 2013, <http://archive.ics.uci.edu/ml>.
  - [21] C.-J. LIN AND J. J. MORÉ, *Incomplete cholesky factorizations with limited memory*, SIAM Journal on Scientific Computing, 21 (1999), pp. 24–45, <https://doi.org/10.1137/S1064827597327334>, <https://doi.org/10.1137/S1064827597327334>, <https://arxiv.org/abs/https://doi.org/10.1137/S1064827597327334>.
  - [22] C.-J. LIN, R. C. WENG, AND S. S. KEERTHI, *Trust region newton method for logistic regression*, Journal of Machine Learning Research, 9 (2008), pp. 627–650.
  - [23] S. MACLACHLAN, T. MANTEUFFEL, AND S. MCCORMICK, *Adaptive reduction-based AMG*, Numerical Linear Algebra with Applications, 13 (2006), pp. 599–620, <https://doi.org/10.1002/>

- nla.486, <http://dx.doi.org/10.1002/nla.486>.
- [24] T. MANTEUFFEL, S. MCCORMICK, M. PARK, AND J. RUGE, *Operator-based interpolation for bootstrap algebraic multigrid*, Numerical Linear Algebra with Applications, 17 (2010), pp. 519–537, <https://doi.org/10.1002/nla.711>, <http://dx.doi.org/10.1002/nla.711>.
- [25] Y. NOTAY, *Flexible conjugate gradients*, SIAM Journal on Scientific Computing, 22 (2000), pp. 1444–1460, <https://doi.org/10.1137/S1064827599362314>, <https://doi.org/10.1137/S1064827599362314>, <https://arxiv.org/abs/https://doi.org/10.1137/S1064827599362314>.
- [26] Y. NOTAY, *Algebraic two-level convergence theory for singular systems*, SIAM Journal on Matrix Analysis and Applications, 37 (2016), pp. 1419–1439, <https://doi.org/10.1137/15M1031539>, <https://doi.org/10.1137/15M1031539>, <https://arxiv.org/abs/https://doi.org/10.1137/15M1031539>.
- [27] Y. NOTAY AND P. S. VASSILEVSKI, *Recursive krylov-based multigrid cycles*, Numerical Linear Algebra with Applications, 15 (2008), pp. 473–487, <https://doi.org/10.1002/nla.542>, <http://dx.doi.org/10.1002/nla.542>.
- [28] C. C. PAIGE AND M. A. SAUNDERS, *Lsqr: An algorithm for sparse linear equations and sparse least squares*, ACM Trans. Math. Softw., 8 (1982), pp. 43–71.
- [29] L. REICHEL AND A. SHYSHKOV, *Cascadic multilevel methods for ill-posed problems*, Journal of Computational and Applied Mathematics, 233 (2010), pp. 1314 – 1325, <https://doi.org/https://doi.org/10.1016/j.cam.2009.03.019>, <http://www.sciencedirect.com/science/article/pii/S0377042709002192>. Special Issue Dedicated to William B. Gragg on the Occasion of His 70th Birthday.
- [30] A. RÉNYI, *On measures of entropy and information*, in Proceedings of the Fourth Berkeley Symposium on Mathematical Statistics and Probability, Volume 1: Contributions to the Theory of Statistics, 1961, pp. pp. 547–561.
- [31] J. W. RUGE AND K. STÜBEN, *Algebraic multigrid*, (1987), pp. 73–130, <https://doi.org/10.1137/1.9781611971057.ch4>, <https://epubs.siam.org/doi/abs/10.1137/1.9781611971057.ch4>, <https://arxiv.org/abs/https://epubs.siam.org/doi/pdf/10.1137/1.9781611971057.ch4>.
- [32] Y. SAAD, *A flexible inner-outer preconditioned gmres algorithm*, SIAM Journal on Scientific Computing, 14 (1993), pp. 461–469, <https://doi.org/10.1137/0914028>, <https://doi.org/10.1137/0914028>, <https://arxiv.org/abs/https://doi.org/10.1137/0914028>.
- [33] Y. SAAD, *Ilut: A dual threshold incomplete lu factorization*, Numerical Linear Algebra with Applications, 1 (1994), pp. 387–402, <https://doi.org/10.1002/nla.1680010405>, <http://dx.doi.org/10.1002/nla.1680010405>.
- [34] Y. SAAD, *Iterative Methods for Sparse Linear Systems*, Society for Industrial and Applied Mathematics, second ed., 2003, <https://doi.org/10.1137/1.9780898718003>, <https://epubs.siam.org/doi/abs/10.1137/1.9780898718003>, <https://arxiv.org/abs/https://epubs.siam.org/doi/pdf/10.1137/1.9780898718003>.
- [35] R. SALAKHUTDINOV AND A. MNIH, *Bayesian probabilistic matrix factorization using markov chain monte carlo*, in Proceedings of the 25th International Conference on Machine Learning, ICML '08, New York, NY, USA, 2008, ACM, pp. 880–887, <https://doi.org/10.1145/1390156.1390267>, <http://doi.acm.org/10.1145/1390156.1390267>.
- [36] J. SIMM, A. ARANY, P. ZAKERI, T. HABER, J. K. WEGNER, V. CHUPAKHIN, H. CEULEMANS, AND Y. MOREAU, *Macau: Scalable bayesian factorization with high-dimensional side information using mcmc*, in 2017 IEEE 27th International Workshop on Machine Learning for Signal Processing (MLSP), Sept 2017, pp. 1–6, <https://doi.org/10.1109/MLSP.2017.8168143>.
- [37] K. STÜBEN, *A review of algebraic multigrid*, in Partial Differential Equations, D. Sloan, E. Süli, and S. Vandewalle, eds., vol. 7 of Numerical Analysis 2000, Elsevier, Amsterdam, 2001, pp. 281 – 309, <https://doi.org/https://doi.org/10.1016/B978-0-444-50616-0.50012-9>, <https://www.sciencedirect.com/science/article/pii/B9780444506160500129>.
- [38] L. N. TREFETHEN AND D. BAU III, *Numerical Linear Algebra*, vol. 50, Siam, 1997.
- [39] A. VAN DER SLUIS, *Condition numbers and equilibration of matrices*, Numerische Mathematik, 14 (1969), pp. 14–23, <https://doi.org/10.1007/BF02165096>, <https://doi.org/10.1007/BF02165096>.
- [40] V. N. VAPNIK, *An overview of statistical learning theory*, IEEE Transactions on Neural Networks, 10 (1999), pp. 988–999.
- [41] P. S. VASSILEVSKI, *Multilevel block factorization preconditioners: Matrix-based analysis and algorithms for solving finite element equations*, Springer-Verlag New York, 2008, <https://doi.org/10.1007/978-0-387-71564-3>.